

Electronic detection of collective modes of an ultracold plasma

K. A. Twedt and S. L. Rolston

*Joint Quantum Institute and Department of Physics,
University of Maryland, College Park, MD 20742, USA*

(Dated: November 10, 2022)

Using a new technique to directly detect current induced on a nearby electrode, we measure plasma oscillations in ultracold plasmas, which are influenced by the inhomogeneous and time-varying density and changing neutrality. Electronic detection avoids heating and evaporation dynamics associated with previous measurements and allows us to test the importance of the plasma neutrality. We apply dc and pulsed electric fields to control the electron loss rate and find the charge imbalance of the plasma has a significant effect on the resonant frequency, in excellent agreement with recent predictions suggesting coupling to an edge mode.

PACS numbers: 52.35.Fp, 52.70.Gw

Collective oscillations are central to the study of plasmas as they embody the rich physics unique to the plasma state and provide diagnostics of plasma density and temperature. Ultracold neutral plasmas (UCPs) [1, 2] are a novel system for the study of collective behavior as they have extremely low temperatures (1-100 K), an inhomogeneous density and are on the border of strong coupling. Like most laser-produced plasmas, UCPs are freely expanding systems and electrons can evaporate out of the plasma at a varying rate determined by external fields, which gives a time-dependence to the neutrality of the system. Previous experiments on UCPs have observed plasma oscillations [3], Tonks-Dattner resonances [4], ion acoustic waves [5, 6] and a high-frequency electron drift instability [7].

Early measurements of plasma oscillations, the simplest collective mode, assumed the electron distribution, n_e , exactly matched the Gaussian ion distribution, n_i [3, 8], ignoring effects of the decreasing neutrality of the plasma as electrons are lost. A recent theoretical study [9] accounted for electron loss and predicted the existence of a zero-temperature mode with a resonant frequency that increases for less neutral plasmas. All theories assumed a spherically symmetric n_e , but we have found there to be a significant asymmetry in typical experiments [10] and the effect of this on electron oscillations has not yet been addressed.

Here, we excite and detect plasma oscillations of a UCP taking into account the changing density, neutrality and symmetry of n_e . We find the variation of the resonant frequency with neutrality agrees with the predictions of [9]. In addition, we have developed a new diagnostic for UCPs where we directly detect oscillations through the current induced on a nearby electrode. We find this method to be more accurate than previous measurements based on enhanced electron emission and we can use it when charged particle detection is not possible.

We create a plasma by two-photon ionization of about 10^6 metastable Xe atoms collected in a magneto-optical trap [11]. The initial plasma density is roughly Gaus-

sian with an rms radius of 0.3 - 0.6 mm. The initial energy given to the electrons, E_e , is controlled by tuning the energy of the ionization laser above the ionization limit. After creation, the plasma loses a few percent of the electrons until a sufficient charge imbalance exists to trap the remaining electrons, forming a plasma. The plasma expands, driven by thermal electron pressure; n_i remains Gaussian, following a self-similar expansion [12] described by $\sigma_i^2(t) = \sigma_i^2(0) + v_0^2 t^2$, where σ_i is the rms radius of the ion distribution and the expansion velocity is typically $v_0 = 50 - 100$ m/s, determined by E_e .

Two wire mesh grids located 1.4 cm on either side of the plasma apply a weak electric field (5-10 mV/cm) that directs evaporating electrons out of the plasma region and onto a microchannel plate detector. A typical electron current signal including the prompt loss of electrons and the electron evaporation during expansion is shown in Fig. 1.

UCPs are small systems, consisting of only $10^4 - 10^9$ ions and electrons and sizes of 0.1 mm to 1 cm, so available experimental probes have been limited. Optical absorption and fluorescence imaging of the plasma ions [13, 14] has provided spatially resolved density and velocity measurements of the ions. Information about the electrons has predominantly been obtained by monitoring the loss rate on a charged particle detector as described. This method of electron detection has succeeded in observing plasma oscillations [3, 4], but only indirectly by applying a constant driving field that resonantly heats the electrons and observing an enhanced loss rate. Thus the measurements are subject to the dynamics involved with heating the electrons and their subsequent evaporation.

We present a new approach to studying electron resonances in UCPs by directly measuring changes in the rf field. Measurements of rf absorption are commonplace in low density laboratory plasmas. Most analogous to our system are measurements of zero-temperature oscillations done on nonneutral plasmas trapped in Penning traps [15-18]. These plasmas are typically of sim-

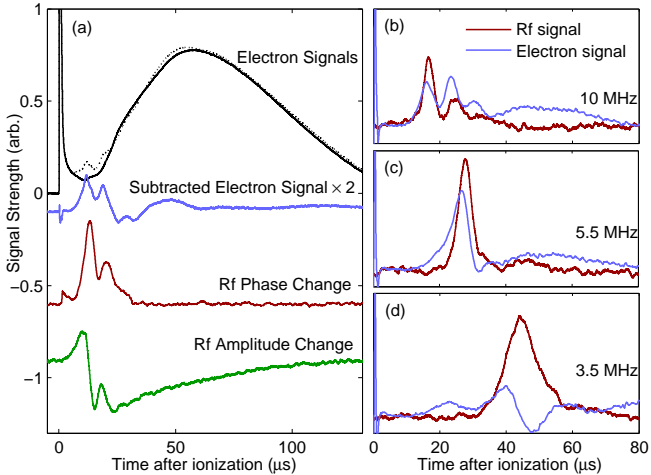


FIG. 1. Comparison of rf signals to electron signals. (a) The dotted and solid black lines are the electrons signals with and without a $f = \omega_{rf}/2\pi = 14$ MHz rf field applied. The rf signals have been rescaled by the same arbitrary factor, and are offset for clarity. (b)-(d) Rf phase change compared to subtracted electron signal for three different frequencies.

ilar size and density to our neutral plasmas, but our rapidly expanding plasmas are untrapped so the measurements must be made during the fast time evolution of the plasma density. Our resonances last only a few μs , about 100 times shorter than the averaging times used for nonneutral plasmas.

The modes are detected by applying a weak, continuous rf drive at frequency ω_{rf} to the grid located above the plasma and monitoring the amplitude and phase changes of the voltage coupled to the symmetric grid below, V_b , as sketched in Fig. 2. In the absence of a plasma, V_b is constant in time and simply related to the electrode geometry. When a plasma is present and driven near a resonant frequency, the oscillation of the plasma induces a current on the bottom grid that interferes with the background signal. The signal from the plasma is much smaller than the background, so we observe only small changes in the amplitude and phase of V_b as the plasma density quickly scans through resonance with the driving field. The results of both quadratures of this homodyne measurement are shown in Fig. 1. Only the relative change in the signal due to the plasma is shown. All measurements are done with ≥ 400 kHz bandwidth, sufficiently large to capture the fast changes in the rf signals. Due to this large bandwidth and small particle number, the signal-to-noise ratio on a single experimental shot is often less than 1, so all plots are an average of at least 150 shots.

The shapes of the signals can be understood by modeling the plasma as a series RLC oscillator in close analogy with [15]. For this work, we note only that the resonance time is associated with a peak in the phase change signal, and thus we will focus on this signal in the remainder of

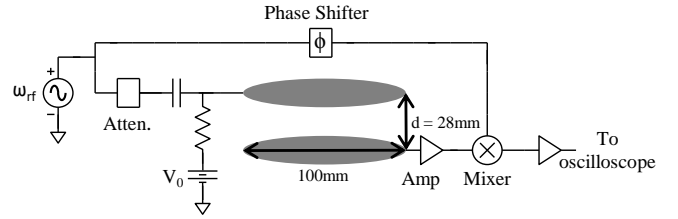


FIG. 2. Schematic for homodyne detection of plasma oscillations.

the analysis. A detailed model could provide information about mode damping and the electron temperature.

Figure 1 shows the comparison of the rf measurements with the enhanced electron emission. The resonance times in the two methods agree to within 1 μs in most cases, after correcting for a delay due to finite bandwidth. The rf measurement is more direct and can be used in experiments where electron detection is complicated or impossible. For large plasmas, we routinely see multiple peaks in the electron emission signal, previously identified as Tonks-Dattner resonances [4], but we typically see only the first two in the rf signal. For larger driving amplitude we can resolve a third peak in the rf signal, but it is a factor of 10 or more smaller in amplitude than the first peak. We anticipate that a higher signal-to-noise measurement would allow us to see all of the modes. Molecular dynamics simulations [19] have also found multiple peaks in the rf absorption in UCPs, but a detailed understanding of these modes is still lacking. Here, we focus only on the zero-temperature plasma resonance, which is the earliest-time feature in both the electron emission and rf signals.

To understand the resonance time, we consider the full picture of the spatial distribution of electrons. Optical measurements of the plasma ions have shown that n_i remains Gaussian throughout expansion [12]. At the center of the plasma, n_e must be nearly equal to n_i , but electron loss ensures deviations at the plasma edge. Bergeson and Spencer [8] solved the cold plasma fluid equations for a perfectly Gaussian electron density ($n_e = n_i$ in all space), assuming no electron loss, and found only a single quasi-mode with a maximum energy absorption at a frequency $\omega = 0.24\omega_{p0}$, where $\omega_{p0} = \sqrt{e^2 n_{e0}/m_e \epsilon_0}$ and n_{e0} is the central plasma density. But even early in the plasma lifetime the charge imbalance may be non-negligible, owing to the prompt loss of electrons at plasma creation (Fig. 1). Lyubonko *et al.* [9] allowed for electron loss by treating n_e as a truncated Gaussian with the truncation radius set by the charge imbalance $\delta = (N_i - N_e)/N_i$, where N_i and N_e are the number of ions and electrons. For plasmas with any significant charge imbalance ($\delta \geq 5\%$), they found a mode where the majority of energy was absorbed near the sharp edge of the cold electron distribution. The relative frequency of the edge-mode resonance,

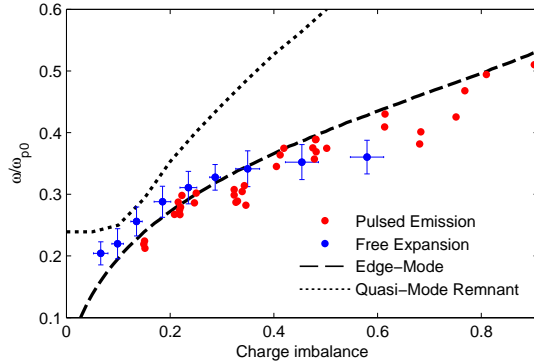


FIG. 3. Edge-mode theory compared to free expansion and pulsed emission data. The edge-mode and quasi-mode remnant curves are from [9]. Blue points with error bars are the average of many free expansion measurements. Red points are individual measurements after pulsed electron emission. Results are the combination of many experimental runs all with $E_e/k_b = 100$ K and $6 \times 10^5 < N_i < 10^6$.

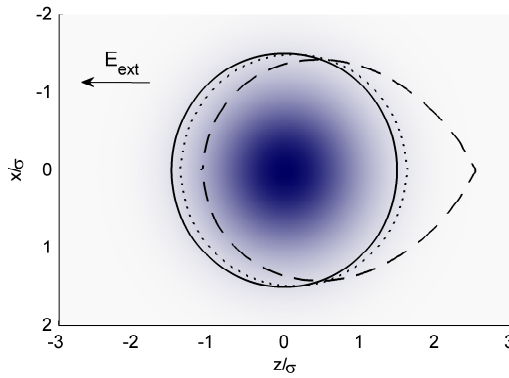


FIG. 4. Electron distributions with $\delta = 0.47$. The shaded region represents the Gaussian ion distribution. Cold electron distributions match n_i inside the boundary lines and drop sharply to zero outside. The solid line is the symmetric electron boundary, the dashed line is the asymmetric boundary during unperturbed plasma expansion and the dotted line is the electron boundary after a pulsed dump of electrons.

$\omega_{rel} = \omega/\omega_{p0}$, increases with δ as shown in Fig. 3.

These theories assume spherical symmetry, but we have found that n_e in a freely expanding plasma can develop a strong asymmetry from the influence of externally applied or stray dc electric fields. To facilitate electron detection, we intentionally apply a small dc field. This field perturbs n_e , which we have used to explain the observed rate of electron loss from our system [10]. The difference between our calculated n_e and the symmetric case for the same charge imbalance is shown in Fig. 4.

We perform two types of experiments to test the edge-mode prediction. First, we record the resonance times from the rf signal, as in Fig. 1, for different ω_{rf} . For smaller ω_{rf} , the resonances are observed later in time, corresponding to a lower density. But due to the contin-

uous electron loss, later time also corresponds to larger charge imbalance, which should increase the relative resonant frequency. Examples of rf signals are shown in Fig. 1 compared to the electron signal for different ω_{rf} .

We note that the electron evaporation signal becomes less reliable at low ω_{rf} . This signal measures evaporation caused by rf heating, but we should not expect a linear relationship between energy absorption and electron emission. As the heating begins and electrons are lost, the plasma potential well deepens, so a greater input energy is needed to subsequently maintain the same electron flux. This effect is most evident at low frequencies as the plasma response becomes much broader in time. By contrast, the rf signal is measuring an induced current that is directly proportional to the amplitude of electron oscillations.

We fit a Gaussian to the first peak of the rf signals to get the resonance time. We independently measure the plasma expansion velocity and ion number, which allows us to calculate the relative resonant frequency ω_{rel} . The charge imbalance is calculated by integrating the electron signals. Only a small 10-15 mV/cm electric field is needed to collect all plasma electrons on our detector. The fraction of the integrated current that arrives before the resonance times gives the charge imbalance δ . The results are shown in Fig. 3.

In a second experiment we dump electrons from the plasma with short voltage pulses of 0.5-2 μ s, chosen to be longer than the electron collision time. This gives control over δ and creates an n_e that is closer to the symmetric distribution used in theory. Fig. 5 shows examples of the electron emission signal with pulses applied.

Before the voltage pulse, we assume a Gaussian n_i and an asymmetric n_e as in Fig. 4. After the pulse, the remaining electrons will be concentrated mostly at the center of n_i . The dc electric field will still polarize the plasma, but the electrons are now held in a deep well and there are not enough to reach the edge of the ions. Electron emission ceases for 10 to 20 μ s. As the plasma continues to expand, the well depth decreases and n_e slowly becomes less symmetric until it again reaches the edge of n_i and electron emission returns. We can calculate n_e after a pulse using the same algorithm used in [10] but fixing the value of δ . An example result is shown in Fig. 4.

The drop in N_e must affect the ion expansion, as the ions outside of the electron cloud are free to move in response to both the external field and their own interactions without electron screening. For larger electron dumps, the density of free ions is large enough that a significant Coulomb explosion occurs and disrupts the following neutral plasma expansion. The electron emission following a pulsed emission is an indicator of the effect of this Coulomb explosion on the plasma. Since the rate of electron emission is related to the size and shape of the ion cloud, an electron emission signal very similar to

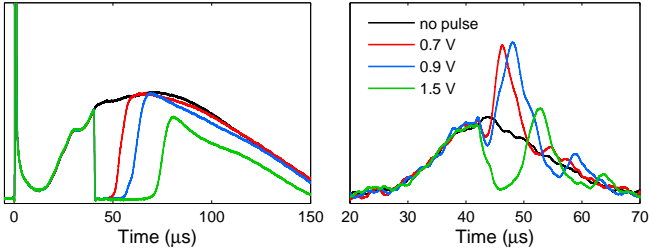


FIG. 5. Electron signals (left) and rf signals (right) with a voltage pulse of $1\ \mu\text{s}$ length and varying amplitude applied at $40\ \mu\text{s}$. The applied frequency is $f = 4\ \text{MHz}$.

the unperturbed expansion indicates a minimal change in plasma expansion, and as shown in Fig. 5 we can for lower voltages get excellent agreement in the late-time emission signals.

For a given voltage pulse, we adjust ω_{rf} and look for resonances in the rf signal during the dead time of the electron emission, as shown in Fig. 5. When we are near a resonance, a clear peak is observed that we identify as the edge-mode resonance. Changing the strength of the voltage pulse dumps more electrons, increasing δ , but leaves all other parameters unchanged. We see that this direct change in charge imbalance increases the time of resonance, which corresponds to an increase in ω_{rel} as predicted.

The data in Fig. 3 are created by applying voltage pulses at many times during expansion. At each time, we sweep ω_{rf} to find resonance peaks that come just after the pulsed emission. We calculate ω_{rel} from the resonance time assuming an uninterrupted ion expansion, and we only plot points where the observed peak comes within $7\ \mu\text{s}$ of the end of the voltage pulse. To get to higher δ we wait until later time in the expansion, letting the plasma naturally lose more charge, before applying the pulse. During pulsed emission, we pulse the electrons away from the detector but still collect all other electrons. The charge imbalance is found by comparing the integrated current after the time of resonance to the full integrated current in the unperturbed experiment.

It is clear from Fig. 3 that the free expansion and pulsed experiments agree with each other and the edge-mode theory. Agreement in the free expansion data is worst at large δ , but these rf signals are very broad, spanning 10s of μs , which increases the uncertainty in fitting a specific resonance time. There are also significant changes to the plasma density and collision rates and significant electron loss during the response time, which may affect the magnitude of the rf signal. The pulsed emission experiments give us control over δ , and we can more easily probe large values. It is unclear why the rf signal after a pulsed emission has a stronger and sharper response than during the normal free expansion.

The importance of the shape of n_e is also not imme-

diate clear. During free expansion, we expect n_e to be asymmetric, like the dashed line of Fig. 4, while the distribution after pulsed emission should be more symmetric. Yet both measurements seem to agree equally well with the perfectly symmetric theory, suggesting that the spatial distribution of charge is only of secondary importance to the integrated amount of charge. It seems surprising that the position of the electron cloud edge is not a larger factor given the finding in [9] that the large majority of energy is absorbed at this edge. It would be interesting to see how the solution of the cold plasma fluid equations changes for the asymmetric distributions of Fig. 4.

In conclusion, we have shown detailed measurements of cold plasma oscillations in an expanding ultracold plasma with a time-varying n_e . Both of our experimental approaches support an increase of resonance frequency with charge imbalance, in agreement with a zero-temperature theory. We have also presented a new diagnostic tool for probing oscillations in ultracold plasmas that is more accurate and more versatile than the previous method.

An important feature of our new measurement is that it allows us to probe electron properties through their resonant behavior without the need for charged particle detection. This advantage was evident in our ability to observe resonances during the dead time in electron emission. Charged particle detection is also prevented when a magnetic field is applied transverse to the axis of the electric grids. We have observed upper hybrid resonances in this setup, which will be the subject of future work.

We have, in some regimes, also been able to observe the free decay of electron oscillations after abruptly turning off the rf drive. Studying mode damping should provide information on the collision properties and electron temperature in UCPs. It is worth noting that we observe plasma resonances at much later times than are normally studied in UCPs. At $90\ \mu\text{s}$, the plasma density has dropped to $2 \times 10^5\ \text{cm}^{-3}$, but we can still observe clear collective behavior, which is a testament to the extremely low electron temperature, expected to be less than 1 K at that time.

We thank A. Lyubonko, T. Pohl and J. M. Rost for helpful discussions and R. A. Perrotta for technical assistance. This work was supported by the NSF PHY1004242.

- [1] T. Killian, T. Pattard, T. Pohl, and J. Rost, Physics Reports **449**, 77 (2007).
- [2] T. C. Killian and S. L. Rolston, Physics Today **63**, 46 (2010).
- [3] S. Kulin, T. C. Killian, S. D. Bergeson, and S. L. Rolston, Phys. Rev. Lett. **85**, 318 (2000).
- [4] R. S. Fletcher, X. L. Zhang, and S. L. Rolston, Phys. Rev. Lett. **96**, 105003 (2006).

- [5] J. Castro, P. McQuillen, and T. C. Killian, Phys. Rev. Lett. **105**, 065004 (2010).
- [6] P. McQuillen, J. Castro, and T. C. Killian, J. Phys. B **44**, 184013 (2011).
- [7] X. L. Zhang, R. S. Fletcher, and S. L. Rolston, Phys. Rev. Lett. **101**, 195002 (2008).
- [8] S. D. Bergeson and R. L. Spencer, Phys. Rev. E **67**, 026414 (2003).
- [9] A. Lyubonko, T. Pohl, and J.-M. Rost, ArXiv e-prints (2010), arXiv:1011.5937 [physics.plasm-ph].
- [10] K. A. Twedt and S. L. Rolston, Phys. Plasmas **17**, 082101 (2010).
- [11] T. C. Killian, S. Kulin, S. D. Bergeson, L. A. Orozco, C. Orzel, and S. L. Rolston, Phys. Rev. Lett. **83**, 4776 (1999).
- [12] S. Laha, P. Gupta, C. E. Simien, H. Gao, J. Castro, T. Pohl, and T. C. Killian, Phys. Rev. Lett. **99**, 155001 (2007).
- [13] C. E. Simien, Y. C. Chen, P. Gupta, S. Laha, Y. N. Martinez, P. G. Mickelson, S. B. Nagel, and T. C. Killian, Phys. Rev. Lett. **92**, 143001 (2004).
- [14] E. A. Cummings, J. E. Daily, D. S. Durfee, and S. D. Bergeson, Phys. Rev. Lett. **95**, 235001 (2005).
- [15] D. J. Wineland and H. G. Dehmelt, J. Appl. Phys. **46**, 919 (1975).
- [16] C. S. Weimer, J. J. Bollinger, F. L. Moore, and D. J. Wineland, Phys. Rev. A **49**, 3842 (1994).
- [17] M. D. Tinkle, R. G. Greaves, and C. M. Surko, Phys. Plasmas **2**, 2880 (1995).
- [18] M. Amoretti *et al.*, Phys. Plasmas **10**, 3056 (2003).
- [19] A. Lyubonko, T. Pohl, and J. M. Rost, Private communication.